Korean J. Chem. Eng., **27**(2), 487-493 (2010)
DOI: 10.1007/s11814-010-0160-4

Studies on the modeling of a molten carbonate fuel cell (MCFC) 5 kW class stack

Sung-Yoon Lee*, Hee-Chun Lim, and Gui-Yung Chung*,†**

*Department of Chemical Engineering, Hong-Ik University, 72-1 Sangsudong, Mapogu, Seoul 121-791, Korea
**Korea Electric Power Research Institute (KEPRI), 103-16 Munjidong, Yuseonggu, Daejon 305-380, Korea
(*Received 24 October 2009 • accepted 7 January 2010*)

Abstract−A mathematical model was developed to simulate the performance of a molten carbonate fuel cell (MCFC) 5 kW class stack. In the modeling calculations, the average current densities of each cell were adjusted to be same for all cells in the stack. In this procedure the operating voltages of each cell were decided. Temperatures of matrixes with an electrolyte increased to a maximum value at the 7th cell. Because the temperatures of the 1st and 9th cells were lower than those of the other cells, the operating voltage of these cells was lower than those of the other cells. Compared to the measured temperature distributions, the calculated results were quite low near the gas entrance. The measured data of the temperature of the matrixes with an electrolyte and the power were estimated well with the modeling calculations. The current density distributions in all cells from the model calculations were similar.

Key words: MCFC, Stack, Mathematical Modeling, Data Fitting, Temperature Distributions, Current Density Distributions, Voltage Distributions

INTRODUCTION

An MCFC stack normally operates at approximately 650°C. The operation at such a high temperature is advantageous for the system in terms of the production of high quality waste heat and fuel flexibility. In addition, typical MCFC operating temperatures produce sufficiently fast electrochemical kinetics that noble metal catalysts are not required for the electrochemical oxidation and reduction processes. The most important model of the MCFC was proposed by Selman [1]. Currently, many mathematical models have been developed using this model; however, most of these researches were carried out on unit cells. Additionally, since they used CFD programs for analysis, they could not include the details of electrochemical reactions. In this research, the large-scale MCFC stack was modeled including the details of electrochemical reaction.

In the previous researches, most of the modeling was done after assuming voltages of each cell in the stack were the same. However, in this research, the voltages of each cell were obtained independently. The MCFC stack is composed of many unit fuel cells connected in a series. In the modeling of a unit cell of MCFC, the current density distribution is calculated at the operating cell voltage. If the areal average value of the distribution is the same as the operating current density, the modeling is done all right. Hence, the modeling of an MCFC stack can be done in the same way after assuming cell voltages. However, there is one constraint that should be kept in the modeling of the stack: the average values of the current density distribution in each cell should be same for all nine cells, since the nine unit cells in the stack are connected in a series. In this research, how this point could be satisfied was studied with the modeling of the MCFC 5 kw class stack.

†To whom correspondence should be addressed.
E-mail: gychung@hongik.ac.kr

MATHEMATICAL MODELING

In MCFC, the anode and cathode electrochemical reactions are as follows [4].

$$\text{(anode) } H_2+CO_3^{2-}\rightarrow CO_2+H_2O+2e^- \tag{1}$$

$$\text{(cathode) } CO_2+\frac{1}{2}O_2+2e^-\rightarrow CO_3^{2-} \tag{2}$$

Besides these reactions, H_2 is generated by the water-gas shift reaction in the anode electrode.

$$CO+H_2O\leftrightarrow CO_2+H_2 \tag{3}$$

The water-gas shift reaction reaches equilibrium at 650 °C to produce H_2. The equilibrium relationship for this reaction is obtained as a function of temperature [5].

1. Mass Balance Equations

The mass balances of anode and cathode gases with Faraday's law are as follows [5].

$$\frac{1}{\Delta y}\frac{\partial(n_a^k X_\alpha^k)}{\partial x}+\nu_{E,\alpha}\frac{j^k}{2F}+\nu_{S,\alpha}\frac{n_S^k}{\Delta x\Delta y}=0 \tag{4}$$

$$\frac{1}{\Delta y}\frac{\partial(n_c^k X_\beta^k)}{\partial x}+\nu_{E,\beta}\frac{j^k}{F}=0 \tag{5}$$

Here, n_a^k and n_c^k are the molar flow rates of gases at x and y in the anode and the cathode gas channels in the k-th cell [molh^{-1}], X_a^k and X_β^k the fractional compositions of the anode and cathode gases, Δy the unit width of a finite element [m], and F the Faraday's constant, 26.8 Ahmol^{-1}. $\nu_{E,\alpha}$, $\nu_{E,\beta}$, and $\nu_{S,\alpha}$ are stoichiometric coefficients in the anode (Eq. (1)) and the cathode (Eq. (2)) electrochemical reactions and the water-gas shift reaction (Eq. (3)), respectively. The water-gas shift reaction is included only in the anode gas. n_S^k [molh^{-1}] is the molar rate of generation or consumption of hydro-

gen in the water-gas shift reaction in the volume ($\Delta x \Delta y b_g$).

The local equilibrium relationship for the water-gas shift reaction (Eq. (3)) is expressed with the local values of partial pressures or compositions of anode gas [7].

$$K^k_{Sx,y} = \frac{(P^k_{H_{2x,y}})(P^k_{CO_{2x,y}})}{(P^k_{H_2O_{x,y}})(P^k_{CO_{x,y}})} = \frac{(X^k_{H_{2x,y}})(X^k_{CO_{2x,y}})}{(X^k_{H_2O_{x,y}})(X^k_{CO_{x,y}})} \quad (6)$$

$$= 157.02 - 0.4447T^k_{x,y} + 4.2777\text{x}10^{-4}T^{k\ 2}_{x,y} - 1.3871\text{x}10^{-7}T^{k\ 3}_{x,y} \quad (2 \text{ at } 650\ ^oC) \quad (7)$$

Here, $T^k_{x,y}$ [K] is the local anode gas temperature at x and y in the k-th cell.

2. Energy Balance Equations

The energy balance equations are written for the separator, the anode gas, the matrix with an electrolyte, and the cathode gas in each cell of the MCFC stack [8,9].

Energy balance for the upper separator in the k-th cell:

$$\frac{\partial^2 T^k_s}{\partial x^2} + \frac{\partial^2 T^k_s}{\partial y^2} = \frac{h_{r,e,s}}{b_s k_s}(T^k_s - T^k_e) + \frac{h^{k+1}_{r,e,s}}{b_s k_s}(T^{k+1}_e - T^k_s) + \frac{h_{s,ga}}{b_s k_s}(T^k_s - T^k_{ga}) + \frac{h^{k+1}_{s,gc}}{b_s k_s}(T^{k+1}_{gc} - T^k_s) \quad (8)$$

boundary condition 1: at x=0 and L, all y; $\frac{\partial T^k_s}{\partial x} = 0$

boundary condition 2: at all x, y=0 and W; $\frac{\partial T^k_s}{\partial y} = 0$

Here, the left-hand terms are the heat transfer by conduction and the right-hand terms are the radiational and the convectional heat transfers.

Energy balance for the anode gas in the k-th cell:

$$\frac{\partial}{\partial x}(m_a C_{p,ga} T^k_{ga}) = h_{e,ga}(T^k_e - T^k_{ga}) + h_{s,ga}(T^k_s - T^k_{ga}) + \sum_\alpha G_{a\alpha} C_{p,ga,\alpha} b_{ga} T^k_{ga} + \frac{Q^k_s}{\Delta x \Delta y} \quad (9)$$

boundary condition: at x=0 and all y, $T^k_{ga} = T_o$

The heat of the water gas shift reaction (Q_S) is included only for the anode gas. Here, the left-hand term represents the enthalpy change of the gas. The first two terms on the right-hand side are convectional energy transfers. The third term is the enthalpy change due to generation or consumption of each component in the reaction. The energy balance equation for the cathode gas can be written similarly as Eq. (9) without Q_S.

The heat of the shift reaction, Q_S [Jh^{-1}], is as follows.

$$Q^k_{Sx,y} = \Delta H^k_{Sx,y} \cdot \Delta n^k_{COx,y} \quad (10)$$

Here, Δn_{CO} [molh^{-1}] is the consumption rate of CO in the shift reaction. ΔH_S [Jmol^{-1}], the heat of shift reaction, is calculated as a function of local temperature as follows [5].

$$\Delta H^k_{Sx,y} = -9{,}932.5 - 0.515T^k_{x,y} + (3.117\times10^{-3})T^{k\ 2}_{x,y} - (1.05\times10^{-6})T^{k\ 3}_{x,y} \quad (11)$$

Energy balance for the matrix with an electrolyte in the k-th cell:

$$\frac{\partial^2 T^k_e}{\partial x^2} + \frac{\partial^2 T^k_e}{\partial y^2} = \frac{h_{r,e,s}}{b_e k_e}(T^k_e - T^k_s) + \frac{h^{k-1}_{r,e,sc}}{b_e k_e}(T^k_e - T^{k-1}_s) + \frac{h_{e,ga}}{b_e k_e}(T^k_e - T^k_{ga}) + \frac{h_{e,gc}}{b_e k_e}(T^k_e - T^k_{gc}) + \frac{Q^k_E}{b_e k_e} \quad (12)$$

boundary condition 1: at x=0 and L, all y; $\frac{\partial T^k_e}{\partial x} = 0$

boundary condition 2: at all x, y=0 and W; $\frac{\partial T^k_e}{\partial y} = 0$

The heat of the electrochemical reaction (Q_E) is included in the equation. Here, the left-hand terms are conductional heat transfers. The right-hand terms are radiational and convectional heat transfers. The heat of electrochemical reaction, Q_E [Jcm^{-2}], is obtained as follows [9].

$$Q^k_{Ex,y} = i^k_{x,y} \cdot \left(-\frac{\Delta H^k_{Ex,y}}{2F} + V^k\right) \quad (13)$$

Here, $\Delta H^k_{Ex,y}$ [Jmol^{-1}] is the enthalpy change by the electrochemical reaction occurring at x and y of the matrix with an electrolyte in the k-th cell and V^k is the voltage of the k-th cell [5]. The enthalpy change is expressed as a function of temperature as follows.

$$\Delta H^k_{Ex,y} = -57{,}018 - 2.738T^k_{x,y} + (0.474\times10^{-3})T^{k\ 2}_{x,y} + (2.637\times10^{-6})T^{k\ 3}_{x,y} \quad (14)$$

3. Current Density

The current density, affected by the cell temperature and the partial pressures of reactants, can be calculated with the other relevant equations. The relationship between current density (j) and cell voltage (V) is written as follows [10].

$$V^k_{x,y} = (V^k_{cNx,y} - V^k_{aNx,y}) - j^k_{x,y} Z^k_{x,y} \quad (15)$$

Here, the equilibrium potentials of anode and cathode, V_{aN} and V_{cN}, are derived from the Nernst equation.

$$V^k_{aNx,y} = V^{o^k}_a + \frac{RT^k_{x,y}}{2F} \ln\left(\frac{X^k_{aCO_{2x,y}} X^k_{H_2O_{x,y}}}{X^k_{H_{2x,y}}}\right) \quad (16)$$

$$V^k_{cNx,y} = V^{o^k}_c + \frac{RT^k_{x,y}}{2F} \ln(X^k_{cCO_{2x,y}} X^{k\ 1/2}_{O_{2x,y}}) \quad (17)$$

where $V^{o^k}_a$ and $V^{o^k}_c$ are standard potentials, and X's are compositions of each gas. The effective cell resistance, Z in Eq. (15), is expressed as follows.

$$Z^k_{x,y} = R^k_{ohmx,y} + Z^k_{ax,y} + Z^k_{cx,y} \quad (18)$$

Here, the ohmic cell resistance, R_{ohm}, is evaluated as a function of temperature [6].

Polarization resistances (Z_a and Z_c) are obtained by dividing anodic and cathodic overpotentials, η_a and η_c, by current density (j). To quantify the polarizations at the anode and the cathode, Selman [6] reported the following equations.

$$Z^k_{ax,y} = 2\times0.4567\times10^{-7}(p^k_{H_{2x,y}})^{-1.801}(p^k_{CO_{x,y}})^{1.533}(p^k_{CO_{2x,y}})^{-1.480}\exp\left(\frac{13{,}140}{T^k_{x,y}}\right) \quad (19)$$

$$Z^k_{cx,y} = 7.504\times10^{-6}(p^k_{O_{2x,y}})^{-0.43}(p^k_{CO_{2x,y}})^{-0.09}\exp\left(\frac{9{,}361}{T^k_{x,y}}\right) \quad (20)$$

By substituting V_{cN}, V_{aN}, and Z into Eq. (15), the following Eq. (21) is obtained.

$$V^k_{x,y} = (V^{o^k}_a - V^{o^k}_c) + \frac{RT^k_{i,j}}{2F} \ln\left(\frac{X^k_{cCO_{2x,y}} X^{k\ 1/2}_{O_{2x,y}} X^k_{H_{2x,y}}}{X^k_{H_2O_{x,y}} X^k_{aCO_{2x,y}}}\right) - j^k_{x,y} Z^k_{x,y} \quad (21)$$

The local current density can be calculated with the values of the

cell voltage and the gas compositions. Then, the average current density of each cell is the areal average of the local current density.

CALCULATIONS

The schematic diagram of the MCFC stack used in the numerical modeling is shown in Fig. 1. The MCFC stack consists of nine unit cells. A unit cell consists of upper and lower separators, a matrix with an electrolyte, and an anode and cathode electrode. The unit cells are connected in a series. As in Fig. 1, the anode and the cathode gases are co-flow in the x-direction.

Values of dimensions of the MCFC stack and the volumetric flow rate of gases used in the modeling are listed in Tables 1 and 2.

The anode electrode, the matrix with an electrolyte, and the cathode electrode were regarded as one solid plate having one value of thermal conductivity. Gradients of temperature and concentration in the direction of cell height, i.e., z-direction in each cell, were ignored.

In the mathematical modeling, the x-directional length and the y-directional width are divided into 20 elements, respectively.

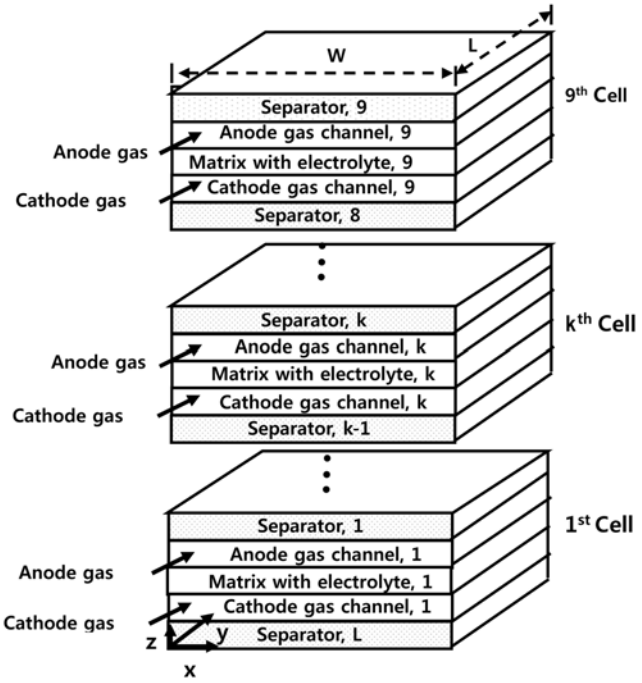

Fig. 1. Schematic diagram of the stack in the parallel flow MCFC.

Table 1. Dimensions of the MCFC 5 kW class stack used in the mathematical modeling

1) Number of cells	(N)	:	9
2) Length	(L)	:	125 cm
3) Width	(W)	:	60 cm
4) Thickness:			
(a) Separator	(b_s)	:	0.2 cm
(b) Gas channel	(b_g)	:	0.17 cm
(c) Anode electrode	(b_{ea})	:	0.08 cm
(d) Matrix with an electrolyte	(b_{em})	:	0.1 cm
(e) Cathode electrode	(b_{ec})	:	0.07 cm

Table 2. Flow rates and compositions of anode gas and cathode gas flowing into the MCFC 5 kW class stack

	Flow rate (mol hr^{-1})	Compositions	
Anode gas	611	H_2	0.8
		CO_2	0.2
Cathode gas	2,150	CO_2	0.3
		O_2	0.15
		N_2	0.55

For each cell in the stack, there are eleven parameters such as voltage (V^k), current density (j^k), compositions of gases (X^k_{aH2}, X^k_{aO2}, X^k_{aCO2}, X^k_{aH2O}, X^k_{cCO2}), temperatures of anode and cathode gases (T^k_{ga}, T^a_{gc}), temperature of the matrix with an electrolyte (T^k_e), and temperature of the upper separator (T^k_s). On the other hand, there are ten available equations. They are five mass balances for anode and cathode gases (Eqs. (4), (5)), four energy balances for the upper separator (Eq. (8)), anode gas and cathode gas (Eq. (9)), and the matrix with an electrolyte (Eq. (12)), and one relationship between the current density and the voltage (Eq. (21)). Since there are ten equations for eleven unknown parameters in each cell, the degree of freedom is one. In other words, one parameter value should be given to calculate the other parameter values. In this modeling, the voltage of each cell in the stack has been assumed and the other parameter values have been calculated with ten equations.

Fig. 2 is the flow diagram for the modeling calculations. Distributions of current density and temperature were calculated with a constant value of the voltage. Conversions by the water-gas shift reaction were calculated with the equilibrium equation, Eq. (6). With these values, gas compositions at every grid point were calculated with Eqs. (4) and (5). In addition, the anode and the cathode polar resistances were calculated with gas compositions at each position. Then, the current density was calculated with Eq. (21). Temperatures of the separator, anode gas, cathode gas, and the matrix with an electrolyte were calculated with the energy balance Eqs. (8), (9), and (12).

The stack is made of unit cells connected in a series. Hence, the current densities of all cells should be the same. This means that the average values of the current density distribution of each cell should be the same for all cells. This condition was met with the following trial and error method.

The current density distributions in each cell were calculated with a certain constant voltage, 0.81 V. Then, the average value of the current density distribution was obtained for each cell. If the obtained average value of a certain cell was different from the operating current density, the voltage of that cell was adjusted. This procedure was repeated until the average current density of each cell became similar to the operating current density for all cells in the stack.

RESULTS AND DISCUSSION

1. The Average Current Density

The operating current density was 0.075 Acm^{-2}. Values of the voltage of each cell decided in the procedure described above are in Fig. 3. The operating voltages of the 1^{st} cell and the 9^{th} cell were adjusted lower than those of other cells. This is because of the lower

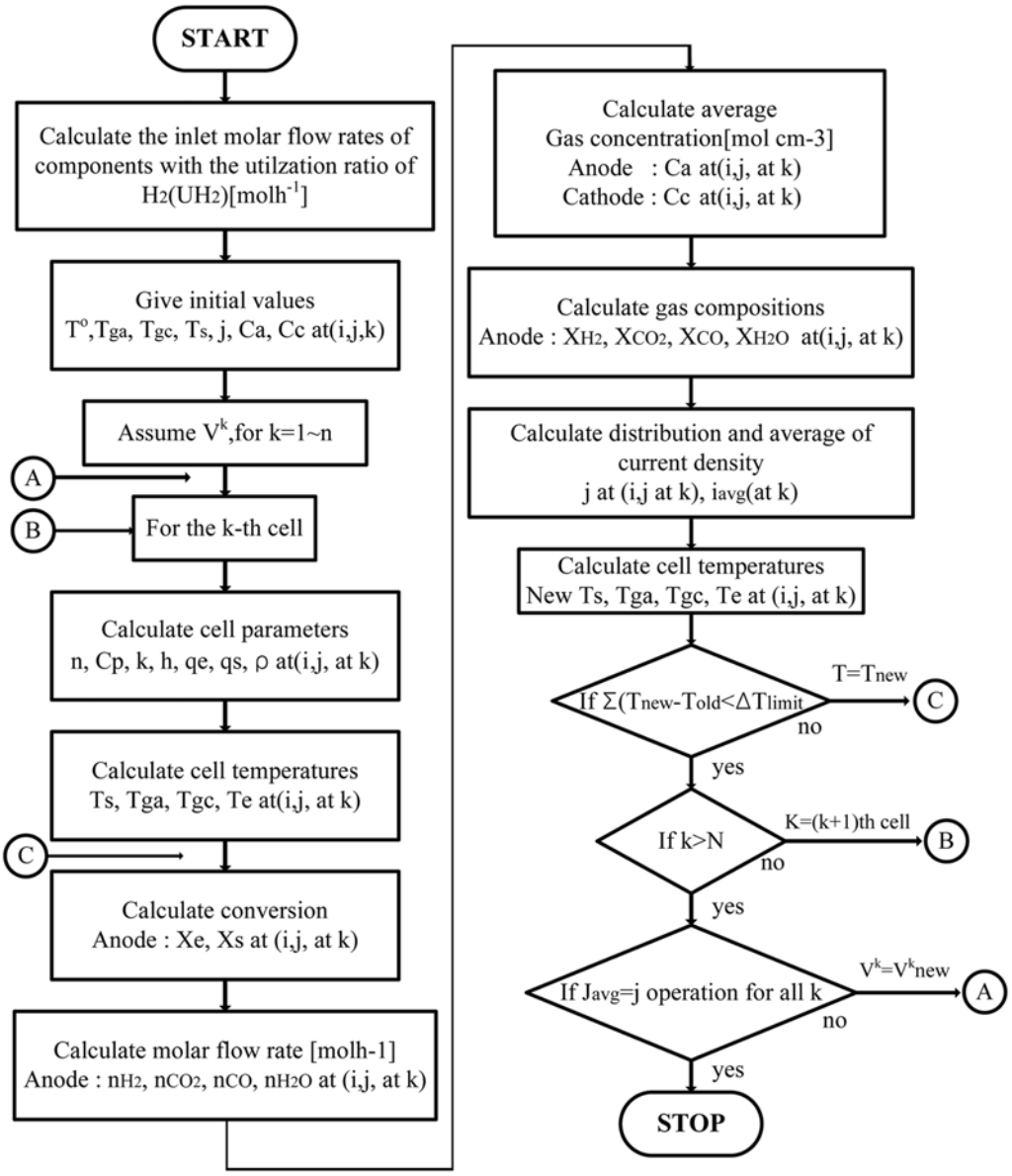

Fig. 2. The flow chart of the numerical modeling calculations for the MCFC 5 kW class stack.

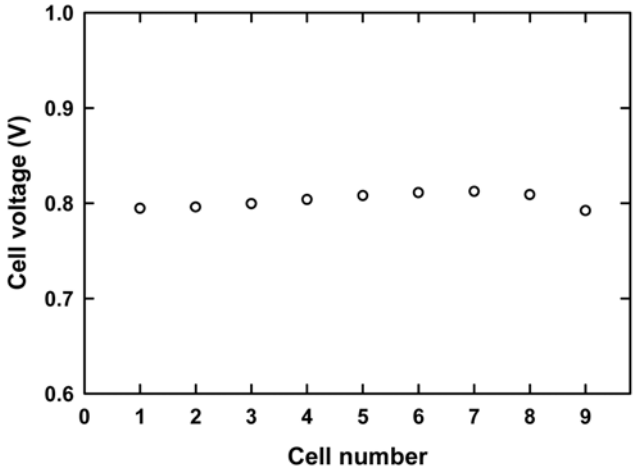

Fig. 3. The voltages of each cell in the MCFC 5 kW class stack.

temperatures of the 1st cell and the 9th cell compared with those of other cells. If temperature of a cell is low, the obtained current density is low due to a slow electrochemical reaction. Therefore, the voltage should be lowered to obtain a higher current density.

The I-V curve of the 5 kW class stack is shown in Fig. 4. The operating voltage and the power were 0.81 V and 4.2 kw at the average cell current density 0.075 Acm^{-2}, respectively. Modeling calculations estimated well the data measured from the real operating fuel cell.

2. Temperature Distributions

Temperature distributions of the matrixes with an electrolyte along the direction of gas flow at y/W=0.5 in the MCFC 5 kW class stack are in Fig. 5. They increase rapidly near the gas entrance due to the high concentrations of fuel gases and the jump of the temperature from the inlet gas temperature to the cell temperature. Then they increase slowly. The temperatures of the matrixes with an electro-

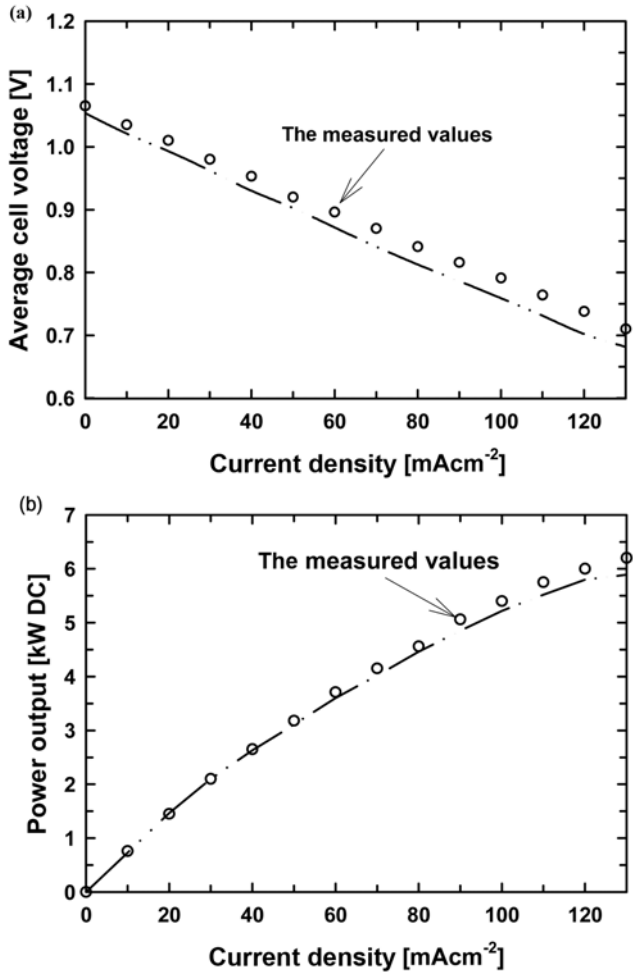

Fig. 4. (a) The I-V curve and (b) the power curve of the MCFC 5 kW class stack. Symbols are data measured from the real operating fuel cell.

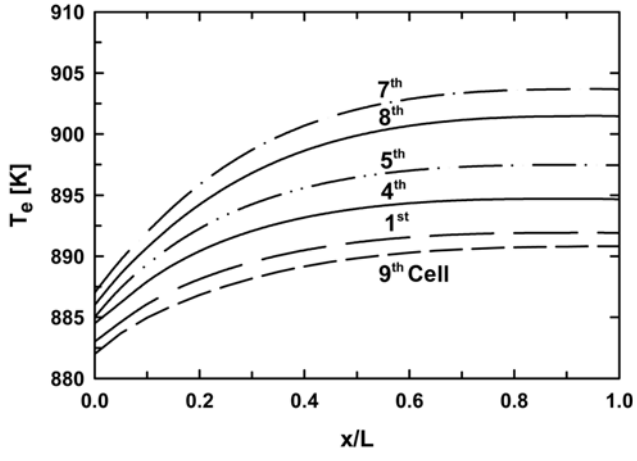

Fig. 5. Temperature distributions of the matrixes with an electrolyte along the direction of gas flow at y/W=0.5 in the MCFC 5 kW class stack.

lyte at the exit are about 10-15 °C higher than those at the entrance. There are almost 5 °C temperature differences between the sides

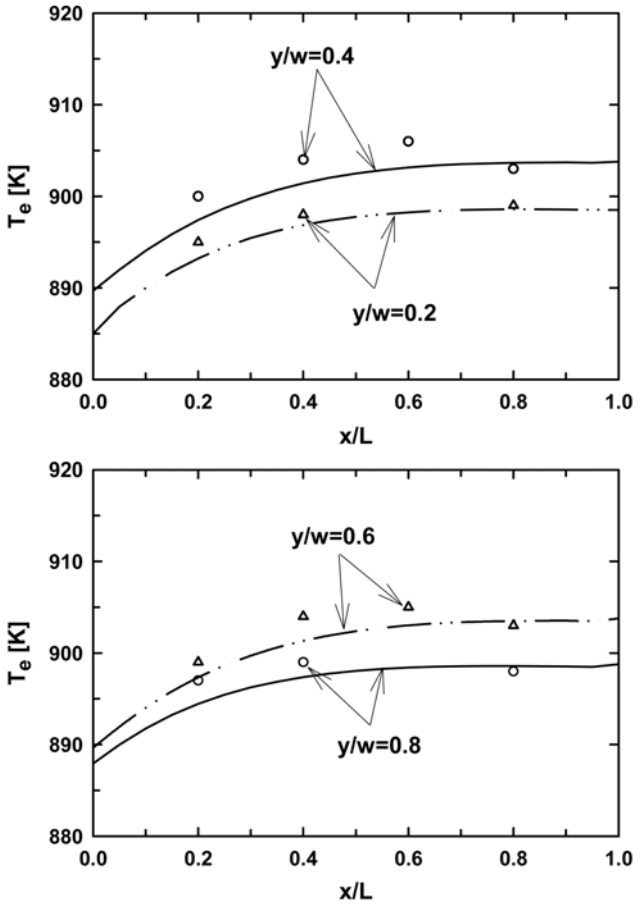

Fig. 6. Temperature distributions of the matrixes with an electrolyte along the direction of gas flow at four different values of y/W in the 7th cell. Symbols are data measured from the real operating fuel cell.

and the center of the MCFC stack.

Since the temperature of the bottom and the top separators is assumed as 605 °C (878 K), the temperatures of the 1st cell and the 9th cell are lower than those of other cells. Hence, along the z-direction, i.e., from the 1st cell to the 9th cell, they increase, reach a maximum value at the 7th cell, and then decrease.

Comparisons between the measured temperature distributions along the direction of the gas flow at different y-values in the 7th real operating cell and those from the modeling calculations are in Fig. 6. Even though the modeling results do not fit well to the measurements of the real operating cell in the inlet part of the gas channel, i.e., x/L=0.2, the overall modeling calculations estimate well those of the real operating fuel cell. The increasing rates of temperatures of the matrixes from the modeling calculations are faster than the measured values of the real operating cell.

3. Current Density Distributions

Current density distributions at y/W=0.5 along the gas flow direction in several cells of MCFC stack are in Fig. 7.

In each cell, the current density distribution is related to the temperature distribution. To observe the effects of temperature on current density, Figs. 5 and 7 were compared. Fig. 5 is the temperature distributions and Fig. 7 is the current density distributions at y/W= 0.5 and along the direction of gas flow.

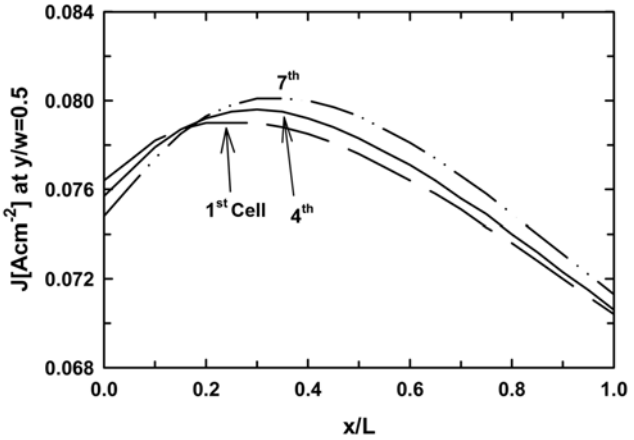

Fig. 7. Current density distributions along the direction of gas flow at y/W=0.5 in the matrixes with an electrolyte of 1st, 4th, and 7th cells in the MCFC 5 kW class stack.

First, at x/L=0.5, changes of current density from the 1st cell to the 9th cell are compared with changes of temperature. Temperatures at x/L=0.5 in Fig. 5 increase from the 1st cell, reach a maximum value at around the 7th cell, and decrease from the 8th cell to the 9th cell. The current densities at y/W=0.5 in Fig. 7 also change in a similar way except at the entrance of the reactant gases.

Second, at y/W=0.5, changes of current density along the gas flow direction in each cell are compared with changes of temperature. Temperatures of the matrix with an electrolyte in Fig. 5 increase continuously along the gas flow direction. However, for all cells in Fig. 7, along the gas flow direction, the current densities increase as the temperatures increase at first and then decrease as the amounts of hydrogen and other gases decrease. In other words, the decreasing gas fractions almost overcome the increasing temperatures after x=0.4L.

As mentioned before, since all cells are connected in series in the MCFC stack, the average values of the current density distribution of each cell should be same for all nine cells in the stack. This means that the average values of the three curves in Fig. 7 should be the same. The shapes of current density distributions in all cells are similar.

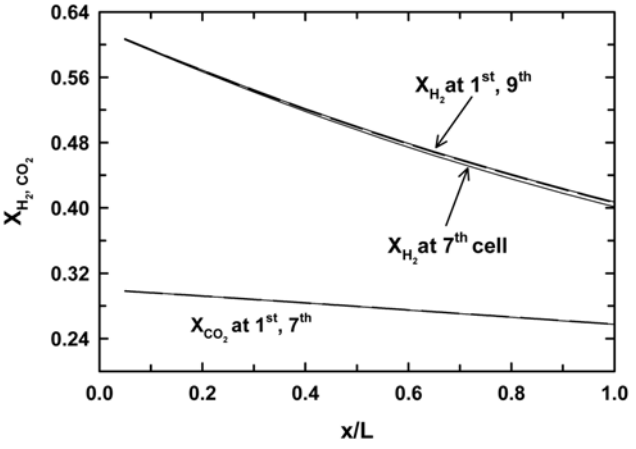

Fig. 8. Distributions of H_2 in the anode gas and CO_2 in the cathode gas along the direction of gas flow in the MCFC 5 kW class stack.

4. Distributions of Gas Compositions

Distributions of the compositions of the anode and cathode gases are shown in Fig. 8. Differences among the compositions in all cells were very small. Due to the consumptions in the electrochemical reactions, hydrogen in the anode gas and carbon dioxide in the cathode gas decrease continuously.

The slope at a certain point of the curve in Fig. 8 is the decreasing rate at that point. Along the gas flow direction, hydrogen decreases fast at first and a little slowly later. Even if differences are very small, the compositions of hydrogen in the 1st cell and the 9th cell decrease a little slowly compared to those in the middle cells. Small decreasing rates mean a slow electrochemical reaction. It can be concluded that hydrogen and carbon dioxide decrease a little slowly because of the low temperatures in the 1st and the 9th cells. Even if differences among the curves of carbon dioxide in Fig. 8 are very small, the trends are similar to those of hydrogen.

CONCLUSIONS

The modeling calculations of an MCFC 5 kW class stack were made considering that the average current densities of each cell should be the same for all cells. The following conclusions were obtained.

To make all the calculated average current densities of each cell 0.075 Acm^{-2}, i.e., the operating current density, the operating voltages of the 1st and 9th cells were adjusted. This is because temperatures of these cells are low compared to those of the 2nd-8th cells. As a result the operating voltage and power were 0.81 V and 4.2 kW, respectively.

Temperatures along the direction of gas flow of the matrixes with an electrolyte increase rapidly near the gas entrance due to the high concentrations of gases and then increase slowly. The temperature of the matrix with an electrolyte at the exit is about 10-15 °C higher than that at the entrance. There are almost 5 °C temperature differences between the sides and the center of the MCFC stack. Temperatures of the matrixes with an electrolyte along the z-direction, i.e., from the 1st cell to the 9th cell, increase and reach a maximum value at around 7th cell. The overall modeling calculations of the temperature distributions estimate well those of the real operating fuel cell.

The current density along the direction of gas flow increases as the temperature increases at first and then decreases as the amounts of hydrogen and other gases decrease. The shapes of current density distributions in all cells are similar.

Even if the differences are very small, the composition of hydrogen in the 1st cell and the 9th cell decreases a little slowly compared with those in the middle cells.

ACKNOWLEDGMENTS

This work was supported by the New & Renewable Energy Program in Korea. The authors acknowledge the financial support of the Korea Ministry of Knowledge Economy through the Electric Power Technology Evaluation and Planning Center and the Korea Electro Power Research Institute (KEPRI). This research was also partially supported by the Korean Council for University Educa-

tion, a grant funded by the Korean Government (MOEHRD) for 2008 Domestic Faculty Exchange, and by the 2007 Hongik University Research Fund.

NOMENCLATURE

b : thickness [cm]
C_p : heat capacity [$Jmol^{-1}K^{-1}$]
F : Faraday's constant [96501 Ceq^{-1} ; 26.8 $Ahmol^{-1}$]
G : moles of gas generated and consumed per unit area [$molcm^{-2}$]
h : heat transfer coefficient [$Jcm^{-2}hK$]
H : molar enthalpy [$Jmol^{-1}$]
j : current density of the cell [Acm^{-2}]
k : thermal conductivity [$Jcm^{-1}h^{-1}K^{-1}$]
m : molar rate [$molcm^{-1}h^{-1}$]
n : molar rate [$molh^{-1}$]
P : pressure [atm]
Q : heat of generation per hour [Jh^{-1}]
R : gas constant [82.06 $cm^3atmmol^{-1}K^{-1}$, 8.314 $Jmol^{-1}K^{-1}$]
R_{ohm} : Ohmic cell resistance [Ω]
T : temperature [K]
V : cell operating potential [V]
V_N : equilibrium potential in Eq. (15) [V]
V^O standard potential [V]
W width of the fuel cell [cm]
x distance in the direction of gas flow [cm]
X mole fraction of the gas component
y distance in the direction of cell width [cm]
Z effective cell resistance [Ωcm^2]

Greek Letters

η : over potential [V]
v : reaction coefficient

Subscripts

a : anode
c : cathode
e : matrix with an electrolyte
E : electrochemical reaction
ga : anode gas
gc : cathode gas
g : gas channel
r : radiation
s : upper separator
S : water-gas shift reaction

Superscript

k : k-th cell

REFERENCES

1. C. Y. Yuh and J. R. Selman, *J. Electrochem. Soc.*, **138**, 3642 (1991).
2. J. Brouwer, F. Jabbari, E. M. Leal and T. Orr, *J. Power Sources*, **158**, 213 (2005).
3. W. H. Chen, M. R. Lin, T. L. Jiang and M. H. Chen, *International J. Hydrogen Energy*, **33**, 6644 (2008).
4. S. W. Nam, T. H. Lim, I. H. Oh, K. S. Lee, S. P. Yoon, S. A. Hong, H. C. Lim, C. W. Lee and Y. K. Sun, *Korean Chem. Eng. Res.*, **33**, 559 (1995).
5. V. Sampath and A. F. Sammels, *J. Electrochem. Soc.*, **127**, 79 (1980).
6. C. Y. Yuh and J. R. Selman, *J. Electrochem. Soc.*, **131**, 2062 (1984).
7. T. L. Wolf and G. Wilemski, *J. Electrochem. Soc.*, **130**, 48 (1983).
8. M. H. Kim, H. K. Park, G. Y. Chung, H. C. Lim, S. W. Nam, T. H. Lim and S. A. Hong, *J. Power Sources*, **104**, 245 (2002).
9. H. K. Park, Y. R. Lee, M. H. Kim, G. Y. Chung, S. W. Nam, S. A. Hong, T. H. Lim and H. C. Lim, *J. Power Sources*, **104**, 140 (2002).
10. J. M. Leo, J. Bolmen and M. N. Mugerwa, *Fuel cell systems*, Plenum Press, New York, 345 (1992).
11. F. Yoshiba, T. Abe and T. Watanabe, *J. Power Sources*, **87**, 21 (2000).
12. F. Yoshiba, N. Ono, Y. Izaki, T. Watanabe and T. Abe, *J. Power Sources*, **71**, 328 (1998).
13. Y. R. Lee, I. G. Kim, G. Y. Chung, C. G Lee, H. C. Lim, T. H. Lim, S. W. Nam and S. A. Hong, *J. Power Sources*, **137**, 9 (2004).
14. T. J. Kim, Y. J. Ahn, J. B. Ju, G. Y. Chung, S. W. Nam, I. H. Oh, T. H. Lim and S. A. Hong, *Energy Eng. J.*, **12**, 354 (1995).
15. Y. J. Ahn, G. Y. Chung, J. B. Ju, S. W. Nam, I. H. Oh, T. H. Lim and S. A. Hong, *Korean Chem. Eng.* Res., **32**, 830 (1994).